

NASA-CR-200122

CASI

14
10
23/10
10

SINGLE CRYSTAL SILICON FILAMENTS
FABRICATED IN SOL: A POTENTIAL IR SOURCE FOR A
MICROFABRICATED PHOTOMETRIC CO₂ SENSOR

FINAL REPORT
(4/95-8/95)
FOR
GRANT NCC2-5054

Juliana Tu
Graduate Research Assistant

and

Rosemary L. Smith
Assoc. Professor

Dept. Electrical & Computer Engineering
University of California, Davis

Submitted to:

John Hines
Sensors 2000!
NASA Ames

The objective of this project was to design, fabricate, and test, single crystal silicon filaments, as potential black body IR sources for a spectrophotometric CO₂ sensing microsystem. The design and fabrication have been reported earlier, but are summarized again here, for completeness. Figure 1 shows the composite layout of the filament die, which contains 4 filaments of different lengths (500 microns, 1 mm, 1.5 mm and 2 mm) and equal widths (15 microns). The composite shows 4 mask layers:

1. Silicon - defines the filament dimensions and contact pads
2. Release Pit - defines the oxide removed from under the filament and hence, the length of the released filament.
3. Pyrex Pit - defines the pit etched in the Pyrex cap (not used)
4. Metal - defines metal pattern on the contact pads / or used as contact hole etch

Figure 2 is a close-up composite view of one filament. The starting material is Bond and Etch Back SOI, BESOI, 4 inch, 100, p-type silicon. The silicon film is 2-2.5 microns thick, and the oxide is 1 micron. The process flow starts with a high temperature (1100 C) boron diffusion of the entire silicon film surface and drive-in (also at 1100 C) resulting in a fairly uniform, boron concentration of $7-9 \times 10^{19} \text{ cm}^{-3}$ throughout the silicon film thickness. This high level of doping results in filament resistances in the .5 - 2 K Ohm range, and is sufficient to prevent significant etching of the filament during subsequent KOH etching. The wafers are oxidized to a thickness of about .1 micron, coated with .3 micron of aluminum and then patterned, photolithographically, to define the filaments (Mask 1). The aluminum, Al, is etched in a standard wet chemical etchant. The Al is then used as the etch mask for the silicon film, which is etched by Reactive Ion Etching (RIE) in an SF₆ + O₂ plasma. After removal of the Al mask, the wafer is repatterned to define the release pit (Mask 2) and the exposed silicon dioxide is then etched in BOE (buffered oxide etch: HF + NH₄F) with nitrogen bubbling, until all of the oxide underneath the filaments has been removed, i.e. the filaments are released from the substrate. Since the filaments are very long relative to the 1 micron gap underneath, they tend to easily stick down onto the substrate, due to both surface tension and due to sagging. In order to ensure both electrical and thermal isolation of the filaments from the substrate, an etch of the exposed silicon substrate in KOH is performed. The etch continues until a pit depth of at least 40 microns is achieved. At this point, the filaments can be electrically tested. Contacts to the filaments were made with needle tips of a micromanipulator stage, or with gold wires which were ultrasonically bonded directly to the heavily doped silicon contact pads.

This remainder of this report summarizes the test results, obtained between April and August, 1995.

I. Device I/V Characteristics

The majority of experimental effort during Spring Quarter (April - June) was spent in coating and I-V testing of the fabricated SOI filaments. The I/V characteristics of the filaments were measured using a DC power supply and multimeter. Typical characteristics are shown in Figure 3. All filaments have similar I/V characteristics, and all have a maximum operating current of about 6.5 mA. Beyond 6.5 mA, the filaments rupture and disintegrate.

The I/V characteristics show that at low applied voltages, the device resistance increases with input bias. This is expected of single-crystal silicon filaments whose resistance has the following relationship:

$$R = \rho * l / (t * w),$$

where ρ = filament resistivity, l = filament length, t = filament thickness, w = filament width

and
$$\rho = (\mu * N * q)^{-1},$$

where μ = carrier mobility, N = carrier concentration, q = carrier charge.

Since carrier mobility decreases with temperature and the carrier concentration is approximately constant with temperature for high doping concentration, at the lower temperatures (or, equivalently, low input voltages), the resultant filament resistance increases with temperature (or voltage).

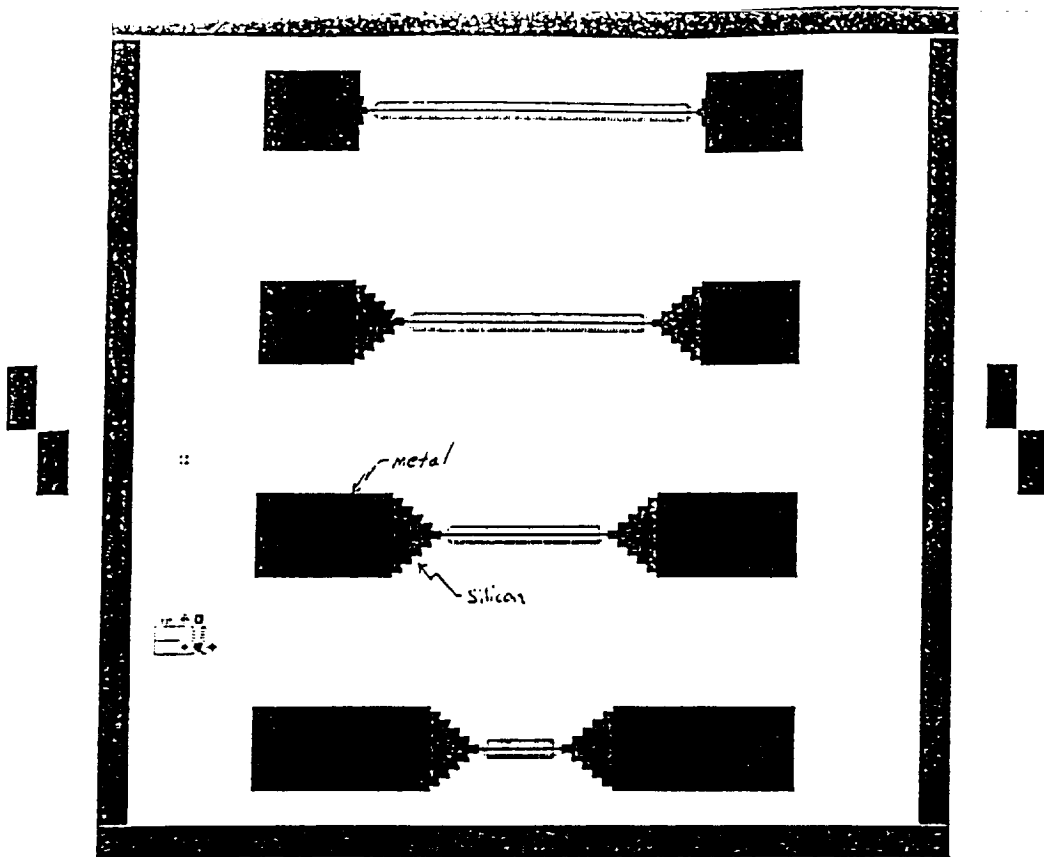


Figure 1 - Composite Layout of Masks for the filament die.
 There are four mask layers: Silicon, Metal, Release Pit, and Pyrex.

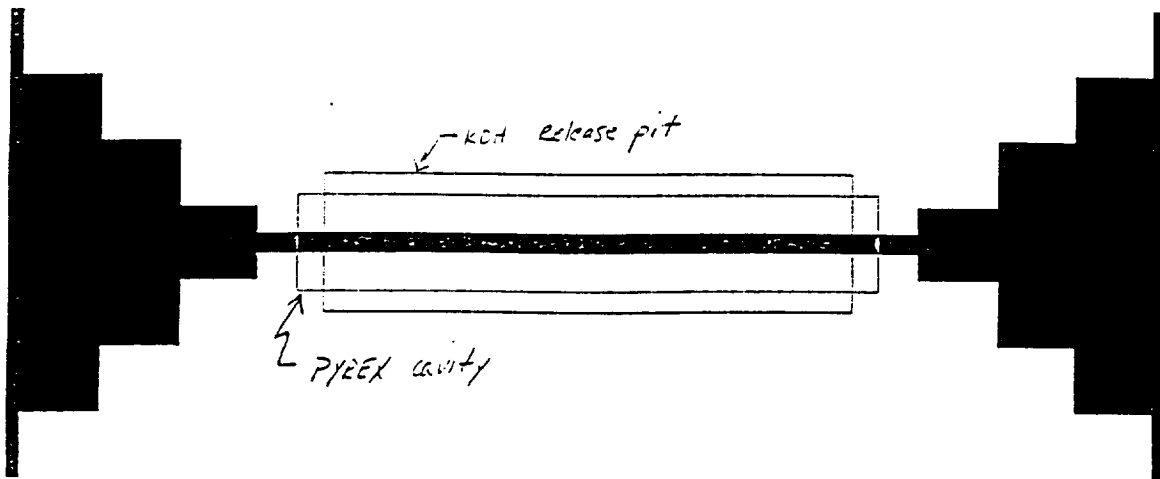


Figure 2 - Enlarged view of composite layout for one filament, showing close-up of the filament, the release pit, and Pyrex cavity (not used) features.

1-mm Filament I-V Characteristics

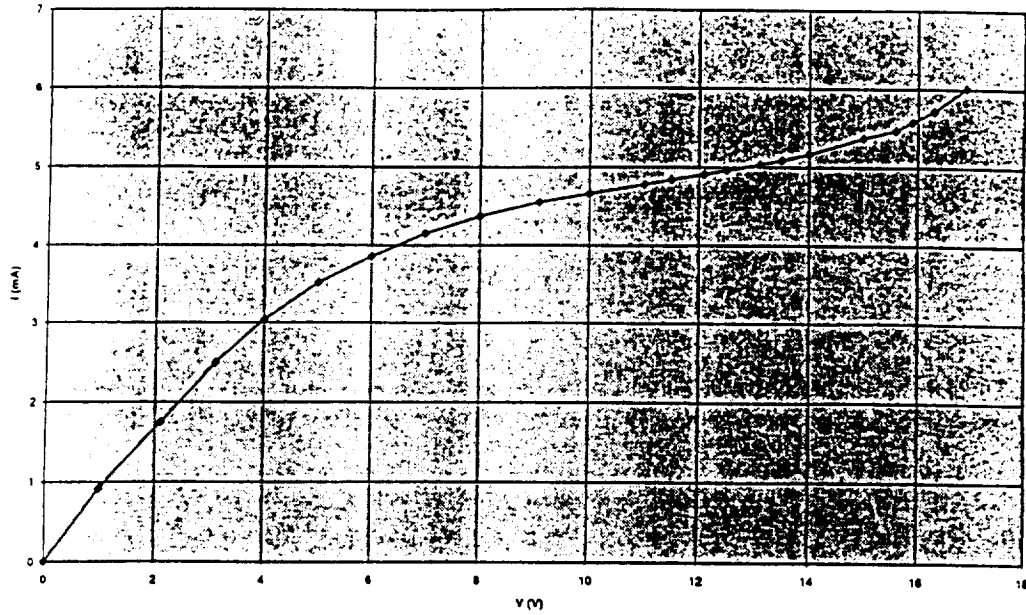


Figure 3 - Typical I-V characteristic of the silicon filaments. Resistance is the inverse slope. It begins to increase above 3 mA, then decreases when the current exceeds 5 mA. Filaments fail above 6 mA (in air).

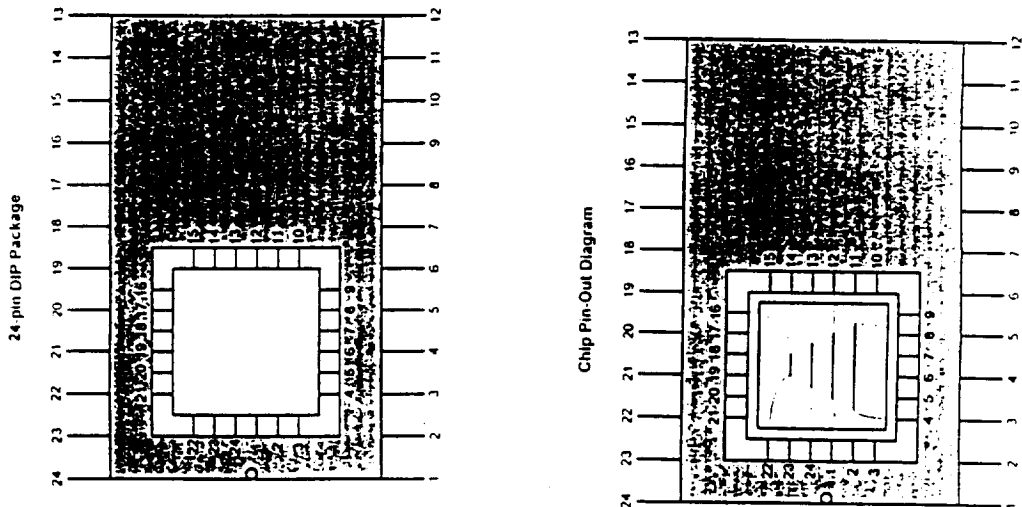


Figure 4 - Package and pin-out scheme used for filament testing.

At higher applied voltages, however, the filament resistance begins to decrease with input bias. This may be due to the fact that the carrier concentration becomes intrinsic at high temperatures (or, equivalently, high input voltages), so that the carrier concentration increases exponentially with temperature. This exponential increase with temperature outpowers the decrease in carrier mobility, which is roughly proportional to $T^{-3/2}$. The resultant filament resistance therefore decreases. Similar I/V characteristics have also been observed in earlier reports on polysilicon filaments [1]

II. Device Coating

To prevent the filaments from oxidation, and therefore, filament resistance instability over long bias times, the filaments were coated so that that filament surface is not exposed to air. Both PECVD and LPCVD nitride coatings were used and compared for this purpose.

A. PECVD Nitride Coating

In this method, the fabricated filament die is first packaged in a 24-pin dual-in-line package (DIP). Gold wire bonds are directly attached to the silicon pads for each filament using a K&S Ultrasonic Ball Bonder. The package and bond layout are shown in Figure 4. This package is then placed in a PECVD furnace and deposited with 2400 Å of PECVD nitride using 55 sccm of NH_3 and 20 sccm of SiH_4 at 300 °C and 30 Watts for 20 minutes.

B. LPCVD Nitride Coating

In this method, the whole wafer with fabricated filaments is coated with 1800 Å of LPCVD nitride (StrataGlass, Inc.). Since the LPCVD deposition is a non-directional process, the free standing filament is coated uniformly on all exposed surfaces. The wafer is then patterned by coating the wafer surface with photoresist, and filling up the release pit with photoresist. The contacts are patterned with Mask 4, and subsequently opened by etching the exposed nitride in RIE in 20 sccm of CF_4/O_2 (CF_4 with 4% O_2) at 200 Watts. The wafer is then stripped of photoresist in an acetone bath, followed by a methanol bath and a DI water rinse. As the last step, the wafer is diced into chips, which are then placed in 24-pin dual-in-line packages, and gold wires are bonded to the exposed silicon pads.

III. Testing

A. Resistance Before And After Coating

The resistance of 0.5 mm filaments, before and after nitride-coating, were measured. For the PECVD-coated filament, the resistance is measured on the package before and after the PECVD nitride is deposited. For the LPCVD-coated filament, the resistance is measured before the filament is deposited with LPCVD nitride and after the filament has been deposited with LPCVD nitride, patterned, diced, and packaged into a chip. The result shows that the resistance of the filament roughly stayed the same after coating.

	R_{before} (k Ω)	R_{after} (k Ω)
PECVD coated chip	0.475	0.476
LPCVD coated chip	0.640	0.645

B. Constant-Voltage Resistance Drift Vs. Time

At high input voltages, the filament resistance drifts with time. The constant-voltage resistance drift was measured for a 1.5-mm LPCVD-coated filament, a 1.5-mm non-coated filament, a 0.5-mm PECVD-coated filament, and a 0.5-mm non-coated filament. For comparison, the filaments are subjected to the same input power for the coated and non-coated filaments. The tests were run under several wattage settings for 10 hours each time. These results are shown in Figures 5 - 8

For the non-coated 1.5-mm filament, we observe a monotonic increase in filament resistance with increasing time. This could be due to thermal oxidation, in air, of the silicon filament, resulting in a reduced cross-sectional area and consequently, an increase in filament resistance. Additionally, at a high constant input voltage, it is possible that the filament gets so hot that more heat is retained in the filament than dissipated into the air, causing the internal filament temperature, and therefore, resistance to increase. (The thermal conductivity of silicon is 0.532 W/cm/K, estimated from Table 1 in [2], while the thermal conductivity of air is 0.057×10^{-3} cal/s/cm/K = 2.39×10^{-4} W/cm/K [3].)

For the LPCVD-coated 1.5-mm filament, the device resistance initially decreases for times close to the origin, then flattens out and stays constant for the remainder of the test period (with the exception that at 133 mW, the resistance drops again after 530 minutes, or almost 9 hours, of operation). The low, resistance drift, at constant voltage, for the LPCVD-coated filament, as compared to the non-coated filament, suggests that the LPCVD coating has reduced the instability problem seen with the non-coated filament possibly by eliminating its susceptibility to rapid oxidation. The initial decrease in the single-crystal resistance may be because, upon passing current through the filament, the LPCVD coating absorbs some of the heat, causing an initial decrease in the filament temperature, and thus the resistance decreases. (The thermal conductivity of LPCVD is 0.03 W/cm/K [1]). As the internal filament temperature stabilizes, the filament resistance remains constant.

Similar results were reported for LPCVD-coated polysilicon filaments [1], where the filament resistance also decreases initially and then flattens for a short period of time. The major difference between the LPCVD-coated single-crystal silicon filaments and polycrystalline silicon filaments is that the resistance of polysilicon filaments eventually increases rapidly, and keeps increasing for the majority of the test period (10 hours), whereas that of the single-crystal filaments stayed constant for the majority of the test period (10 hours). The dramatic constant-voltage resistance drift of the polysilicon filament presents a serious long-term stability problem. The results shown here indicate that single-crystal silicon filaments are much more electrically stable than polycrystal silicon filaments.

The non-coated 0.5-mm filament shows the same characteristics as those of the non-coated 1.5-mm filaments. That is, there is a monotonic increase in filament resistance with increasing voltage stressing time. To compare the resistance drift characteristics with those of the 0.5-mm PECVD-coated filament, the same input powers were applied to both coated and non-coated filaments. At 48 mW and 60.8 mW, the resistance of the PECVD-coated filament remains constant for 10 hours. At 90.6 mW, however, the resistance of the PECVD-coated filament begins a monotonic increase with increasing voltage stressing time. However, at this high input power, the non-coated filament has already burned out.

It is noteworthy to point out that since the resistance drift occurs at fairly high input bias, which is beyond the range of operation needed to have the emission peak at 4.2 μm , both coating methods should work very well for our application.

IV. Alternative Sealing Method

An alternative method for sealing the device from air involves eutectically bonding the fabricated wafer to a gold-coated pyrex-7740 wafer so that the filament is housed in a hermetically sealed environment. The 7740 glass has an etched dome coated with an IR-reflective gold film. The emitted light from the filament is reflected off the IR-reflective coating and transmits through the backside of the substrate. Although long-term drift in sealed-cavity devices using eutectic bonding has also been reported [4], [5], it provides a better seal for the filaments than just the nitride protective coatings. The feasibility of eutectically sealing the device is yet to be demonstrated, and is suggested for future research endeavors.

Constant-Voltage Resistance Drift of 1.5-mm Uncoated Filaments

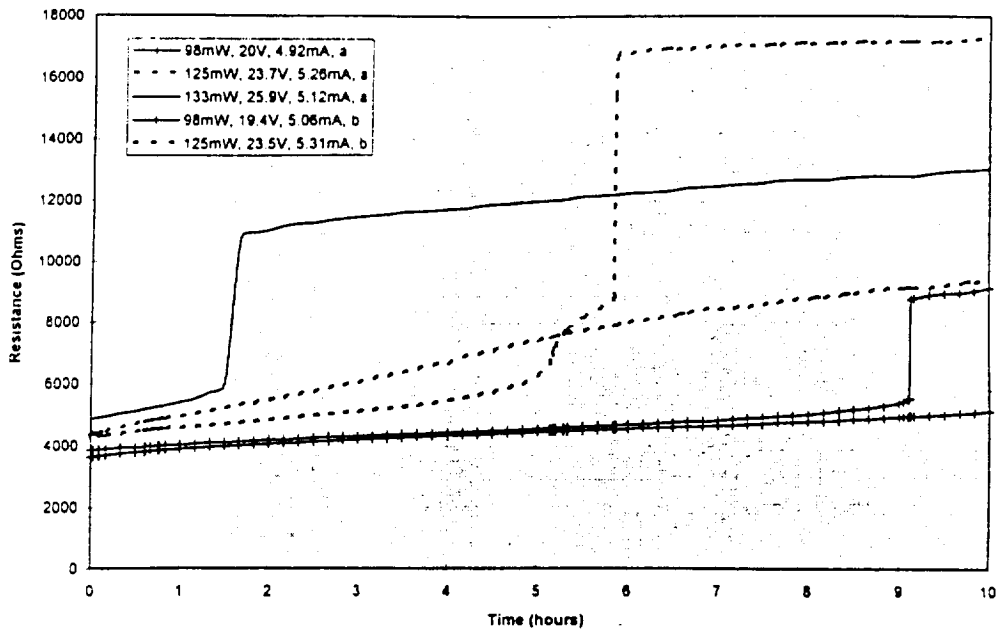


Figure 5 - Filament drift characteristics, in air, uncoated. Two different filaments, both 1.5 mm long, a and b, at different biasing levels: 98 mW, 125 mW, and 133 mW.

Constant-Voltage Resistance Drift of 1.5-mm LPCVD-Coated Filaments

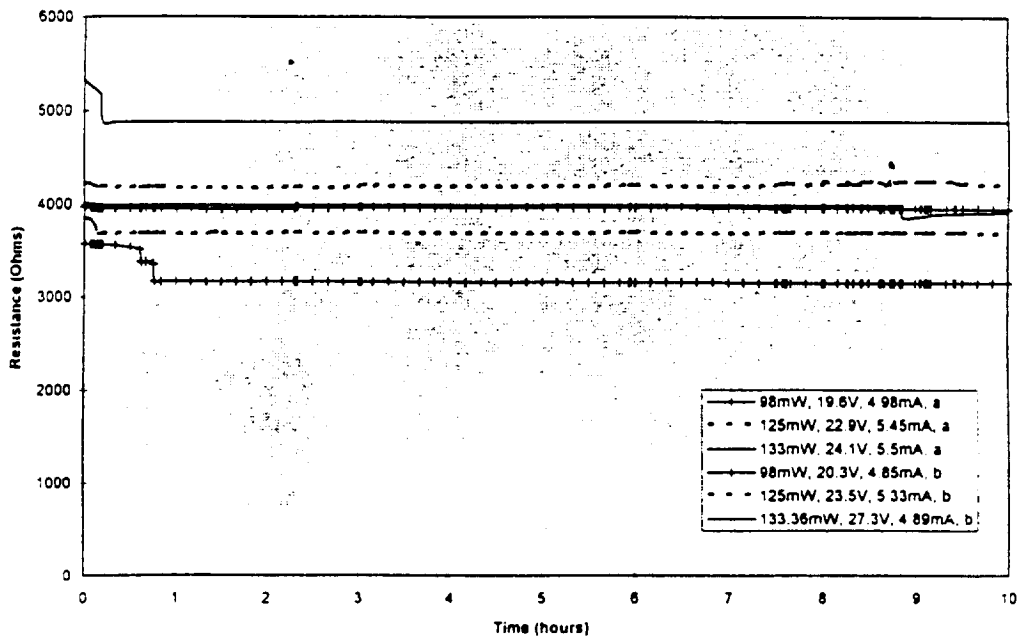


Figure 6 - Filament drift characteristics, in air, coated with LPCVD silicon nitride.

Constant-Voltage Resistance Drift of 0.5-mm Uncoated Filaments

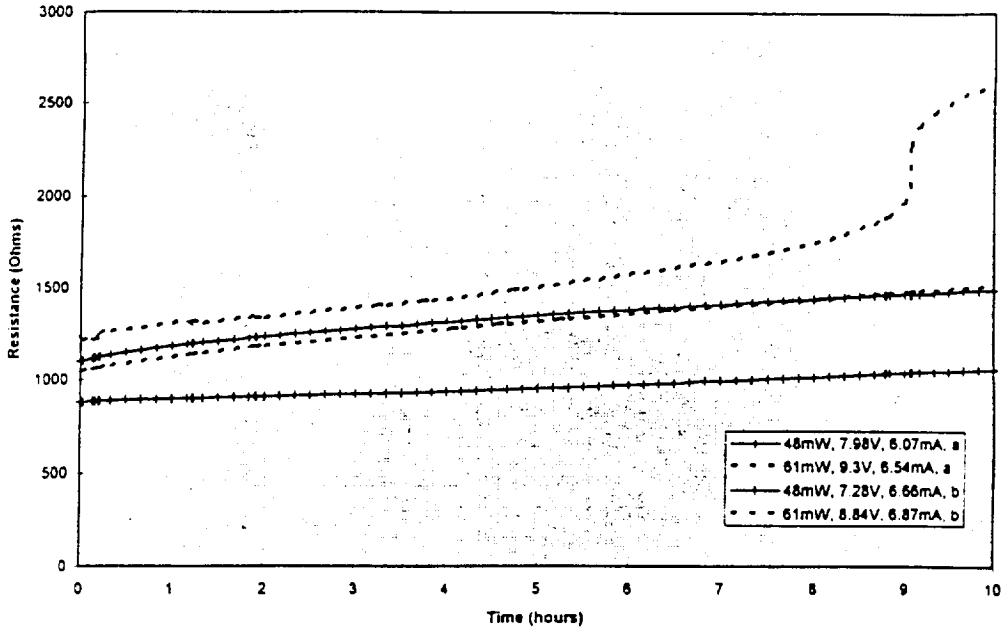


Figure 7 - Filament drift characteristics, in air, uncoated. Two filaments, a and b, at two different power settings: 48 mW and 61 mW.

Constant-Voltage Resistance Drift of 0.5-mm PECVD-Coated Filaments

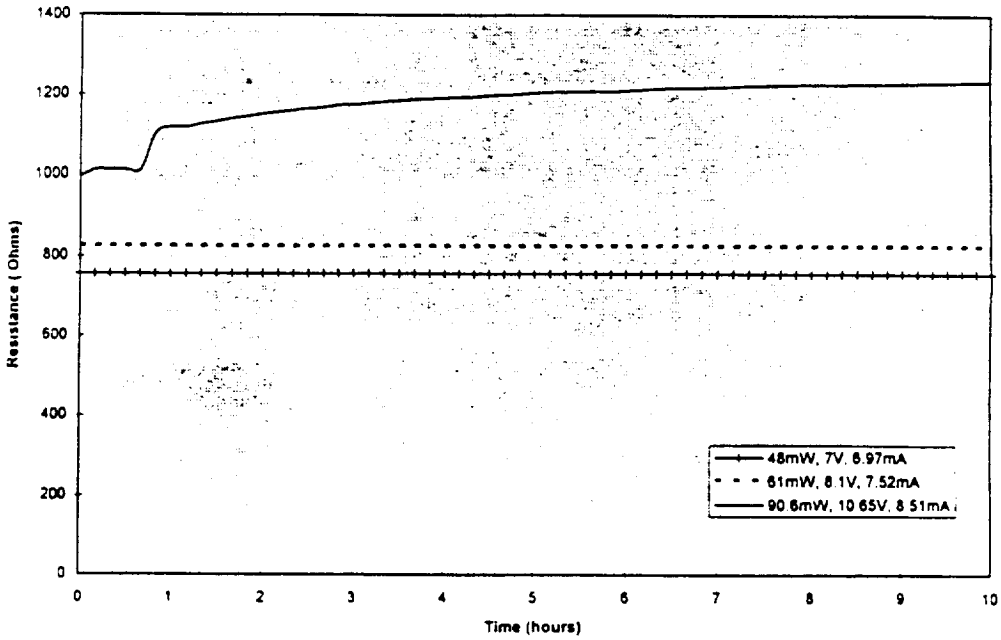


Figure 8 - Filament drift characteristics, in air, coated with PECVD silicon nitride. One filament, same size as in Fig. 7 (.5 mm), at 3 power settings.

V. Emission Characteristics

Packaged, coated filaments were sent to NASA for spectral characterization. At the time of writing this report, we have only the results taken on one filament: 1.5 mm long, non-coated, filament.

A. Measurement Set-up

To get the absolute radiation intensity (vs. relative intensity), the filament radiation characteristics must be compared with a National Physical Laboratory (NPL) blackbody. Figure 9 shows the controlled background flux calibration facility using a NPL blackbody. Figure 10 shows the experimental apparatus used to characterize the optical emission of the filament of this work, with the filament in place of the blackbody in Figure 9.

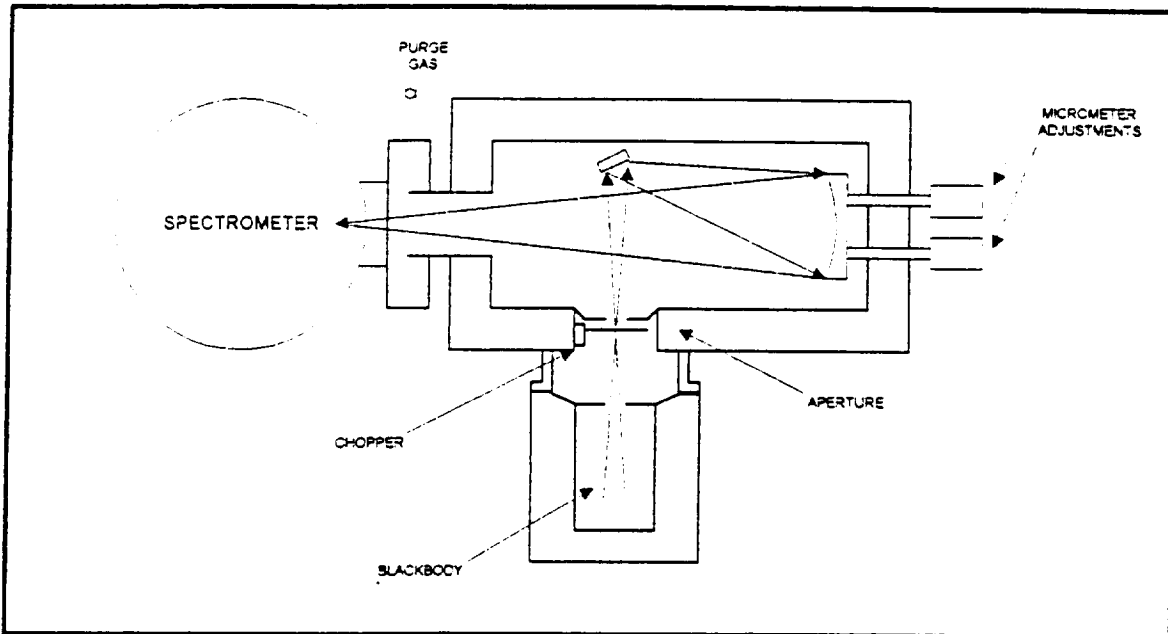


Figure 9: Controlled background flux calibration facility using a NPL blackbody

The packaged filament is placed on a substrate leading to the opening of a nitrogen purged chamber. At the opening of the chamber is a 100 μm aperture that limits the amount of light entering the chamber and a chopper used to chop the signals coming out of the filament. The chopper is needed to distinguish the filament signal from the background signals. The signals are directed by a set of condensing lenses inside the chamber to a spectrometer at the end of the chamber.

B. Radiation Measurement

The spectrum of the filament is compared with a NPL blackbody, whose spectrum is taken using the same apparatus. A relative spectrum relating the spectral intensity of the filament to that of the NPL blackbody is obtained. Figure 11 shows the emission characteristics of a 1.5-mm, uncoated filament in relative spectral intensity as compared with the NPL blackbody.

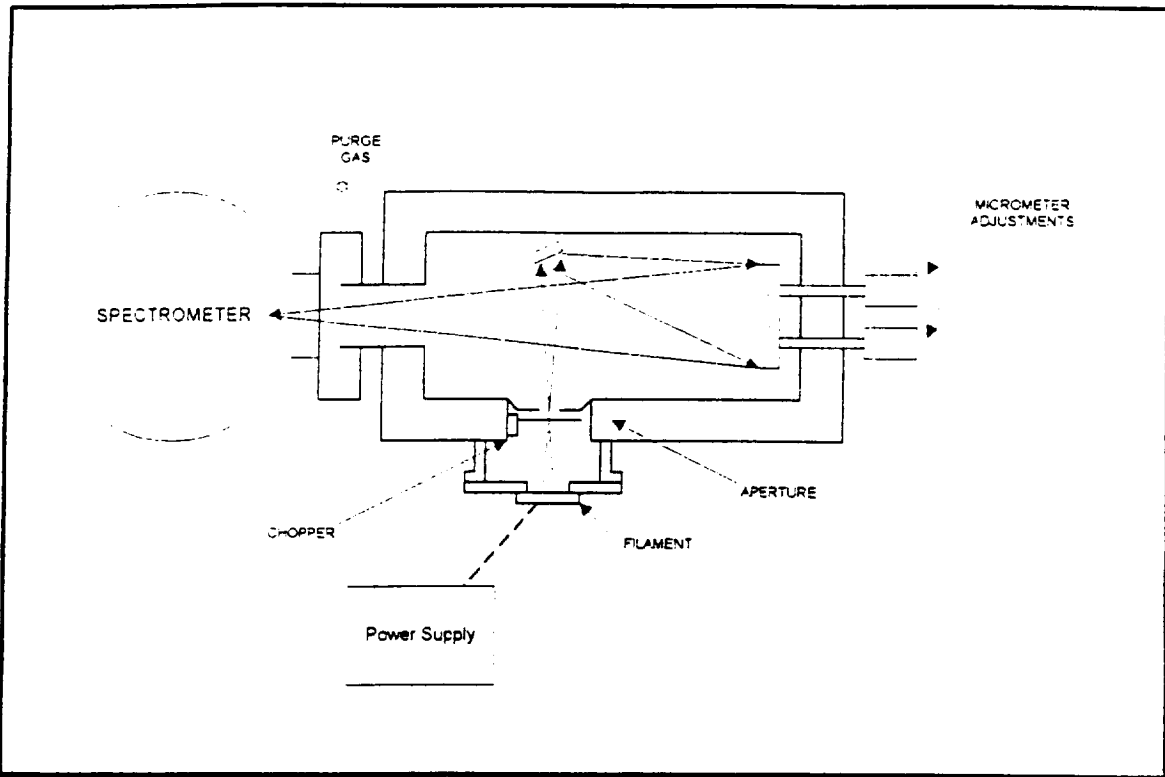


Figure 10: Experimental apparatus for filament emission characterization

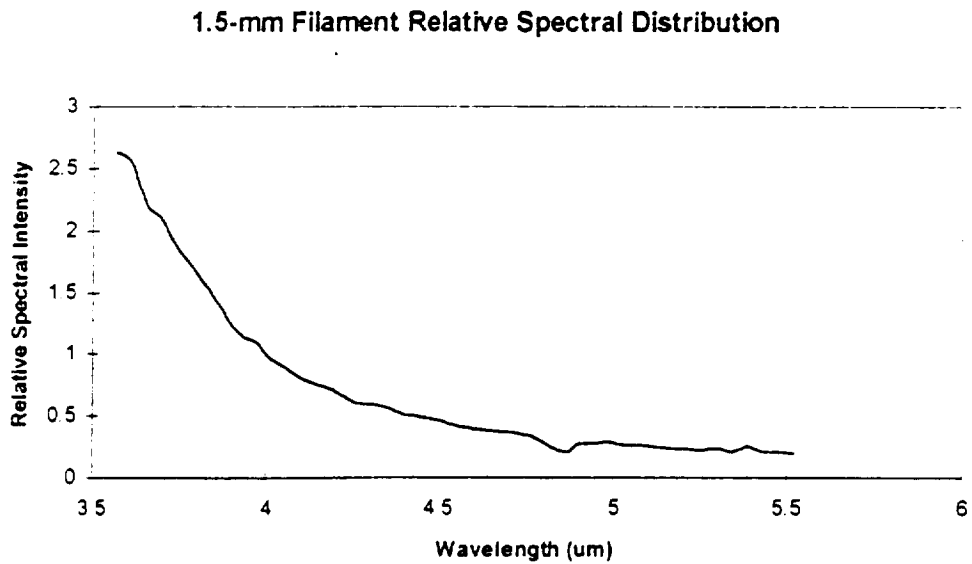


Figure 11: Emission characteristics of a 1.5-mm, uncoated filament in relative spectral intensity as compared with the NPL blackbody. Filament was biased at 20 Volts, 5 mA.

Calibration

In order to obtain the filament spectral intensity on an absolute scale, calibration of the relative spectral data is needed. To calibrate the spectrum of the filament, the absolute spectral intensity of the blackbody is first calculated. An absolute spectral intensity of the filament can then be found using the relative spectrum. The power radiated from the NPL blackbody is [6]:

$$P(\lambda, T) = \frac{W_\lambda}{\pi} A' \quad (\text{eq. 1})$$

where A' is the projected area of the blackbody, and W_λ is the spectral emittance of the blackbody:

$$W_\lambda = \frac{2\pi c^2 h}{\lambda^5 (e^{hc/kT\lambda} - 1)}, \text{ or equivalently,}$$

$$W_\lambda = \frac{c_1}{\lambda^5 (e^{c_2/\lambda T} - 1)}$$

where $c_1 = 3.74 \times 10^{-12} \text{ W-cm}^2$, and $c_2 = 1.4388 \text{ cm-K}$.

Eq. 1 then becomes:

$$P(\lambda, T) = A' \frac{c_1}{\pi \lambda^5} \left[\frac{1}{e^{c_2/\lambda T} - 1} \right] \quad (\text{eq. 2})$$

The blackbody is a "volume" of black material with an F/17 cone leading to the aperture. That is, the cone opens 1 unit for every 17 units it goes out. Since the blackbody is a "volume" of material rather than a planar structure, in order to make a meaningful comparison of the spectrum of the NPL blackbody to that of the filament, we have to first calculate the projected NPL blackbody area, A' , onto the filament plane. Figure 12 shows the geometry of the F/17 cone used in obtaining the blackbody projected area. The distance from the aperture to the filament is 3.75 inches, or equivalently, 9.525cm. The F/17 cone opens at an angle, θ , of 3.37° . The projected circular area of the blackbody has a radius, r .

$$r = 9.525 \text{ cm} \times \tan \frac{\theta}{2} = 9.525 \text{ cm} \times \tan \frac{3.37^\circ}{2} = 0.2802 \text{ cm}$$

The resulting projected blackbody area, A' , is:

$$A' = \pi r^2 = \pi (0.2802 \text{ cm})^2 = 0.2467 \text{ cm}^2. \quad (\text{eq. 3})$$

A close look at the measurement setup diagram (Figure 9) reveals that when the chopper is open, the signal detected (S_o) consists of radiation not only from the NPL blackbody itself, but also from the aperture, which is coated with a black material. When the chopper is closed, the signal detected (S_c) consists of radiation from the aperture and the chopper blade, which is also coated with a black material. If we consider the signal in the closed-chopper (or "off") state as having zero power, i.e., $S_c = 0$, then the signal in the open-chopper (or "on") state can be found by subtracting the detected signals in the two states (Figure 13). That is,

$$\begin{aligned} S &= S_o - S_c \\ &= (S_{\text{NPL}} + S_{\text{aperture}}) - (S_{\text{chopper}} + S_{\text{aperture}}) \\ S &= S_{\text{NPL}} - S_{\text{chopper}} \end{aligned}$$